Nano Biomed. Eng., 2018, Vol. 10, Iss. 1

87

Research Article

Sequential Nucleation Growth of ZnO Nanoflowers

Nora Elizondo[1]✉, Dora Irma Martínez[1], Ana Maria Arato[1], Rodrigo González[2], Francisco Vázquez[3], Gustavo Rodríguez[3], Ernesto Torres[4], Víctor Manuel Castaño[5]✉

[1]Department of Physics, Universidad Autónoma de Nuevo León, San Nicolás de los Garza, N. L., Código Postal: 66455, México.
[2]Civil Engineering Faculty, Universidad Autónoma de Nuevo León, San Nicolás de los Garza, N. L., Código Postal: 66455, México.
[3]Faculty of Mechanical and Electrical Engineering, Universidad Autónoma de Nuevo León, San Nicolás de los Garza, N. L., Código Postal: 66455, México.
[4]Departamento de Inmunología, Facultad de Medicina, UANL, Ave. Dr. José Eleuterio González 235, Col. Mitras Centro, Monterrey, N.L. México, Código Postal: 64460.
[5]Centro de Física Aplicada y Tecnología Avanzada, Universidad Nacional Autónoma de México, Boulevard Juriquilla 3001, Querétaro 76230, México.

✉ Corresponding author. E-mail: nelizond@yahoo.com; vmcastano@unam.mx

Abstract

The morphological characteristics of ZnO nanostructures were systematically studied from dense rods to flower-like shapes. The ZnO flower-like samples were prepared by direct decomposition of a $Zn(OH)_4^{2-}$ precursor and by the sequential nucleation and growth method consisted of a multistep synthesis of complex nanostructured films. Condition-dependent experiments systematically were compared as to reveal the formation and detailed growth process of ZnO nanosized crystallites and aggregates. X-ray diffraction, transmission and scanning electron microscopy indicated that the precursor, solution basicity, reaction temperature and pressure as well as reaction time, were responsible for the variations of the morphologies. ZnO flower-like and large nanorods of exceptional uniformity, orientation alignment, and optical properties have been produced in this work. Several synthesis steps are needed to produce oriented nanostructures that are more complex than simple nanorod architectures. These structures have potential applications in building functional electronics devices and optoelectronic properties.

Keywords: Structural analysis and structural determination; Zinc oxide; Sequential nucleation growth

Introduction

One-dimensional nanometer-sized semiconductor materials, i.e., nanowires and nanorods, have attracted considerable attention due to their great potential for fundamental studies of the roles of dimensionality and size in their physical properties, as well as for their application in optoelectronic nanodevices [1]. Zinc oxide (ZnO), a semiconductor with a direct wide band gap (3.37 eV at room temperature) and large exciton binding energy (60 meV), is one of the most promising materials for the fabrication of optoelectronic devices operating in the blue and ultraviolet (UV) region and for gas sensing applications [2, 3]. The synthesis, characterization and application of various 1D ZnO nanostructures including the rods/wires [4], belts/ribbons [5], rings [6], tetrapods [7], combs [8], sheets [9] and complex structures [10] are presently the subject of intense research.

During the past decades, reports on the synthesis

88

Nano Biomed. Eng., 2018, Vol. 10, Iss. 1

of various structures of ZnO are increasing, including rods [11], wires [12], tubes [13], tower- [14], star- [15], dendrite- [16] and flower-like [17, 18]. These structures are expected to have more potential applications in building functional electronics devices with special architectures and distinctive optoelectronic properties. Therefore, it is desired to synthesize ZnO nano- or microstructures in a controllable shape and size by simple approach to answer the demand for exploring the potentials of ZnO. Unfortunately, up to now, it is still challenging task for material scientists to directly fabricate large-scale ZnO crystals with controlled morphology. The ability to control and manipulate the physical and chemical properties of materials has been one of the challenging issues for chemistry and materials researchers. These properties are strongly related to two crucial geometrical parameters: size and shape. Now, chemists are exploring many ways to obtain such control at the nanometer scale. Various shapes of materials have been synthesized, such as nanotube, nanorod, nanobelt, nanoplate, and nanoparticles, flower-like pattern, etc. Three-dimensional (3D) superstructures composed of 1D and 2D nanoscale building blocks have been the subject of increasing interest in material synthesis and device fabrication because of their unique collective properties and practice applications [19-21]. Self-assembly process is probably the simplest synthetic route to 3D superstructure [22]. The hydrothermal technique is a useful method in preparing nanomaterials and it has been applied to the synthesis of various ZnO nanostructures. The conditions for synthesizing ZnO-nanorod arrays from aqueous solutions were reviewed by Govender et al. [23], and similar aqueous chemical routes have been developed to grow oriented arrays of nanorods and nanotubes of other metal chalcogenides and hydroxides [24-28]. Electrochemical deposition in aqueous solutions has also been applied to directly deposit oriented films of ZnO nanorods [29-34], cuprous oxide nanocubes, nanopyramids [35] and several other crystal habits [36]. To date, most of these solution-phase synthesis methods have produced either continuous film structures or arrays of nanorods or nanotubes. Although a few studies have recently reported tower-, tube-, and flower-like morphologies resulting from the addition of organic growth modifiers [37-39], fabrication of more complex nanostructures, such as those observed in natural materials or biominerals [40], remains a significant challenge.

In this work the morphology and evolution characteristics of ZnO nanostructures were systematically studied from dense rods to ZnO flowers like. The ZnO flowers like were prepared by direct decomposition of a $Zn(OH)_4^{2-}$ precursor and by the sequential nucleation growth method consisted of a multistep synthesis of complex nanostructured films.

Experimental

The ZnO flowers like were synthesized mainly by modification of two methods: the first method is the Direct Method (DM) and the second is the Sequential Nucleation and Growth Method (SNGM), the zinc oxide flowers like were prepared by direct method as follows: 50 mL of an aqueous solution (0.1 mol/L) of zinc nitrate hexahydrate $(Zn(NO_3)_2 \cdot 6H_2O)$ was prepared. 50 mL of an aqueous solution of sodium hydroxide (NaOH) (1.5 mol/L) was also prepared. The NaOH aqueous solution was gradually added to the zinc nitrate aqueous solution. At the beginning of this process, a $Zn(OH)_2$ precipitate was obtained. As more of the NaOH solution was added, the $Zn(OH)_2$ precipitate dissolved to yield a homogeneous clear aqueous solution containing $Zn(OH)_4^{2-}$ ions. The aqueous solution was kept in a polypropylene beaker at 348, 358, 363 or 368 K for 3 h with a rubber stopper to prevent evaporation of the solvent. After this heating procedure, a precipitate was formed. The obtained precipitate was filtered with suction and dried at 348 K for 12 h.

The second method SNGM is a multistep synthesis of complex nanostructured films that begins with substrate preparation for heterogeneous nucleation of oriented nanocrystals, on many substrates, this can be accomplished with self-assembled monolayers (SAMs), but an even more straightforward approach is to seed the substrate with nanoparticles of the desired film material.

The decomposition or hydrolysis of zinc salts is an established route to the formation of ZnO colloids and nanocrystals in aqueous solution. We adapted this approach to form layer of ZnO nanocrystals directly on a substrate by thermally decomposing of zinc acetate at 350-400 °C. In our optimized procedure, a substrate is wet with a droplet of 0.005 mol zinc acetate dehydrate (98%, Aldrich) in ethanol, rinsed with clean ethanol after 10 s, and then blown dry with a stream of argon. This coating step is repeated three to five times. The substrate, now covered with a film of zinc acetate crystallites, is heated to 350 °C in air for

Nano Biomed. Eng., 2018, Vol. 10, Iss. 1

89

20 min to yield layers of ZnO islands with their (0001) planes parallel to the substrate-independent and occurs on flat surfaces regardless of their crystallinity or surface chemistry, including ZnO single crystals. The zinc acetate deposition and decomposition procedure is carried out twice to ensure a complete and uniform coverage of ZnO seeds.

After uniformly coating the silicon wafer with ZnO nanocrystals, hydrothermal ZnO growth was carried out suspending the wafer upside-down in an open crystallizing dish filled with an aqueous solution of zinc nitrate hydrate (0.025 mol) and diethylenetriamine (0.025 mol) in a in a Parr Digestion Bomb model 4748 at 363 °K. Reaction times spanned from 0.5 to 6 h. The wafer was then removed from solution, rinsed with deionized water, and dried. We grew vertical ZnO nanowire arrays from the aligned nanocrystal seeds in an aqueous solution at 90 °C.

We have used several synthesis steps to produce oriented nanostructures that are much more complex that simple nanorod architectures and repeated sequentially the steps before mentioned and the rods were nucleated tree or four times to synthesize the ZnO "flowers like". The desired nanostructures were produced by altering the experimental conditions of DM and SNGM methods by modification of process parameters and by the chemical quality of modification and the quantity of steps in the case of SNGM method.

The zinc oxide "flowers like" also were prepared by modified direct method (MDM) as follows: 30 mL of an aqueous solution (0.1 mol/L) of zinc nitrate hexahydrate ($Zn(NO_3)_2 \cdot 6H_2O$) was prepared. 30 mL of an aqueous solution of sodium hydroxide (NaOH) (1.5 mol/L) was also prepared. The NaOH aqueous solution was added to the zinc nitrate aqueous solution and mixed. The aqueous solution was kept in a Parr Digestion Bomb model 4748 at 363 °K with autogen pressure. Reaction times spanned from 3 to 6 h. After this heating procedure, a precipitate was formed. The obtained precipitate was filtered with suction and dried at 348 °K for 12 h.

Modified Sequential Nucleation and Growth Method (MSNGM), in this case we carried out experiments exactly with the same several synthesis steps like SNGM, the only different thing was that after uniformly coating the silicon wafer with ZnO nanocrystals, hydrothermal ZnO growth was carried out suspending the wafer upside-down in an open crystallizing dish filled with an aqueous solution of

zinc nitrate hydrate (0.025 mol) and diethylenetriamine (0.025 mol) at atmospheric pressure at 363 °K, without using a Parr Digestion Bomb with autogen pressure. Reaction times spanned from 0.5 to 6 h.

The heating time dependence of the precipitated amount of zinc oxide was estimated by heating the aqueous solutions containing $Zn(OH)_4^{2-}$ ions for a period of time between 0 and 6 h and recording the results. 10 mL of the supernatant was separated and the concentration of Zn^{2+} ion was measured by using the EDTA chelate titration method. All of the chemicals used in this preparation were reagent grade (Aldrich®, U.S.A.). Fig. 1 shows a schematic diagram of the entire process.
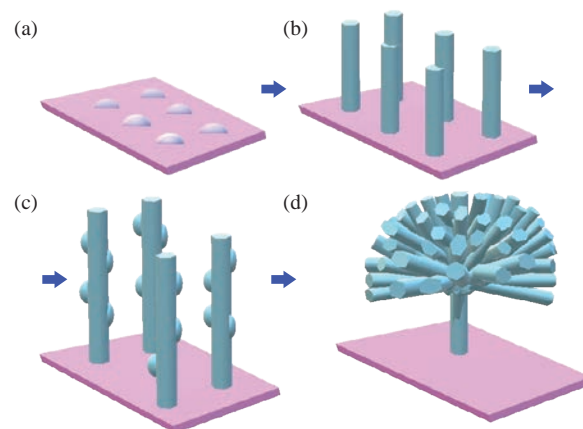

Fig. 1 Schematic diagram of sequential nucleation growth of ZnO flowers: **(a)** Deposition of crystallization seeds of ZnO on substrate; **(b)** Growth of the rods in nucleation center; **(c)** Second nucleation deposition of ZnO seeds on first patterned nanorods; and **(d)** Secondary growth of nanorods on first patterned nanorods to form ZnO flowers.

The morphology of ZnO "flowers like" was studied by scanning electron microscopy (SEM) in a Hitachi S-4500 field emission SEM operating at 5 kV. For crystal structure identification we used a Phillips automated vertical scanning powder diffractometer. The spectra were obtained between 10 and 90 2θ degrees. We used X-ray photoelectron spectroscopy XPS to surface analysis of the ZnO "flowers like".

Transmission electron microscopy (TEM) and associated techniques such as energy dispersive X-ray spectroscopy (EDS), high-resolution electron microscopy (HREM), and high-angle annular dark field (HAADF) were applied to determine the subnanometer structure, chemical composition, and homogeneity of the ZnO "flowers like". For TEM analysis, the samples were sonicated in isopropanol and deposited on lacey carbon on copper grids. TEM analysis was carried out in

a JEOL 2010 F microscope equipped with a Schottky-type field emission gun, an ultra-high-resolution pole piece, and a scanning-transmission unit with a high-angle annular dark-field detector (HAADF) operating at 150 kV.

The structures and the crystalline sizes of the obtained powders were characterized by means of X-ray diffraction (XRD) (Cu-Kα, 40 kV, 200 mA, MXP-18, Bruker AXS Co., Ltd., Kanagawa, Japan). The lattice parameters were measured by using high purity Si crystal powder (99.999%) as an internal standard. An optical system of SS=1°, DS=1°, RS=0.15 mm and a graphite monochrometer was used.

In order to examine the concentration of alkali metal ion in the obtained zinc oxide precipitate, 0.1 g of the completely dried zinc oxide powder was dissolved into 10 mL of HCl aqueous solution (2 mol/L) and the total volume of the solution was adjusted to 100 mL. The concentration of the alkali metal ion in the solution was measured by atomic absorption spectroscopy. The molar ratio of the alkali metal ion in the obtained zinc oxide was less than 0.1% in all the cases.
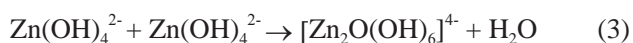
Results and Discussion
Chemical reactions

On the basis on the above-described hydrothermal processes ZnO "flowers like" were obtained. During the reaction, the $Zn(OH)_2$ was formed when the NaOH solution was added in the cases of DM and MDM. Nevertheless, it was dissolved because of the final high ratio $[OH^-]/[Zn^{2+}]$. Under these reaction conditions, the conversion of $Zn(OH)_2$ to $Zn(OH)_4^{2-}$ occurred, according the following equations:

$$Zn^{2+} + 2OH^- \rightarrow Zn(OH)_2 \tag{1}$$

$$Zn(OH)_2 + 2H2O \rightarrow Zn(OH)_4^{2-} + 2H^+ \tag{2}$$

Gradually, under these hydrothermal conditions, the reaction between the $Zn(OH)_4^{2-}$ species leads to form large zinc hydroxide species $ZnxOy(OH)z^{(x+2y-2x)}$, which finally precipitate and form the ZnO, as can be seen by the following equation:

$$Zn(OH)_4^{2-} + Zn(OH)_4^{2-} \rightarrow [Zn_2O(OH)_6]^{4-} + H_2O \tag{3}$$

This reaction mechanism has been explained by Yamabi et al. [41] and Li et al. [42, 43].

Multistep synthesis of complex nanostructured films often begins with substrate surface preparation for heterogeneous nucleation of oriented nanocrystals.

Two-step, seeded growth of simple one dimensional oriented nanocrystalline films and multistage growth of more complicated nanostructures are vanguards for a process to systematically assemble complex, hierarchical crystal architectures [44]. In solution – phase synthesis zinc oxide "flowers like" nanostructures were successfully produced through multistep precipitation of powders in bulk aqueous solutions in the cases of SNGM and MSNGM. We have investigated multistep, aqueous nucleation and growth methods that have produced higher-order ZnO "flowers like". In the hierarchical growth method, the first step was to create nucleation sites, via processes such as seed deposition (Fig. 2(a)). After nucleation process, oriented nanocrystals grow in the 001 plane from these nucleation sites (Fig. 2(b)), and in subsequent reaction steps, new crystal nucleate and grow on the crystals produced in previous stages (Fig. 2(c)-(e)). This provides the capability to build a diverse range of complex nanostructures from various primary subunits have been synthesized with a sequential nucleation and growth process. During the second step, new crystals grow on the surfaces of the primary rods when bifunctional diaminoalkane molecules are added to the solution (Fig. 2(c)). More details of the morphology changes during the synthesis process can be appreciated in the series of SEM micrographs of Fig. 2(d)-(i).

In the third step, the secondary crystals are "healed" to the hexagonal prismatic shape, and in the fourth step, additional branch crystals nucleate from the secondary structures to form ZnO "flowers like" [45].

The creation of new nucleation events that produce crystal growth is a critical step for the success of the multistage approach. Without the diamine molecules, new nucleation is not observed after the primary stage, and repeated crystal growth simply increases the primary crystal size [46].

We developed seeded-growth methods that permit control over the size, population density, and spatial distribution of the ZnO crystals.

The seeds were well deposited on the substrate using many mature techniques, such as dip-/spin-coating, sol-gel coating, or electrophoretic deposition. In most seeding techniques, the nanoparticles are produced in a separate process before physical deposition on the substrate. However, atomic layer deposition, radiofrequency (RF) magnetron sputtering, solution coating, electrochemical deposition, and hydrothermal
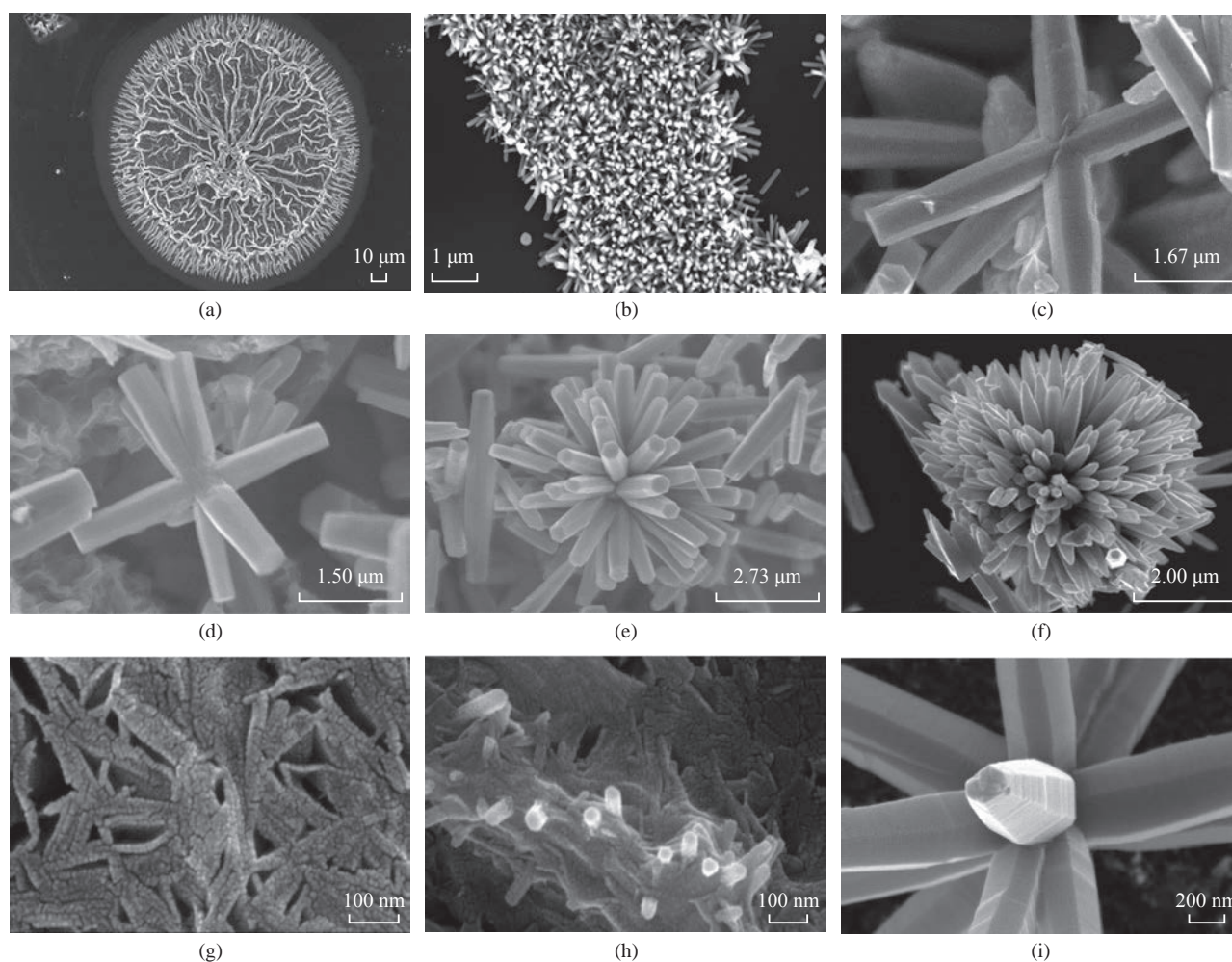
Fig. 2 Synthesized zinc oxide **(a)** seed, **(b)** rods, **(c)** first nucleation, **(d)** second nucleation, **(e)** flower like by sequential nucleation growth method, **(f)** flower like by direct method, **(g)** morphology just before the rods start to grow, **(h)** growth of some rods at the beginning of the process, and **(i)** details of one of the flower, showing the growth bands.

pre-treatment produce a nanoparticle seed layer during an initial deposition step by hydrothermal method as can be seen from Fig. 2. Once the seed layer is formed, oriented nanocrystal growth follows in a second step (Fig. 2(b)). These two-step processes hint at the potential of using multiple reaction steps to control nanostructured-film synthesis [47] as can be seen from Fig. 2(c)-(e). The synthesis of flower like by direct method can be seen in Fig. 2(f).

Fig. 3 shows scanning electron micrographs of ZnO "flowers like" synthesized by MSNGM and MDM.

The changes in the concentration of the solutions and the parameters of the processes induced changes in the kinetics of the crystal growths than, in turn can change the final morphology of the ZnO "flowers like" as can be seen from Fig. 2 and 3. The petals of the flowers had different ends in agreement with Fig. 2(e), the ZnO "flowers like" synthesized by the SNGM

has in the end of the transversal section of the petals, hexagonal prismatic shape and these petals grow in the direction 0001. From Fig. 3(a) and (b) the ZnO "flowers like" were synthesized by MSNGM and can be seen that the petals of the flowers end in a reduced hexagonal prismatic shape, they grow in the direction 0001 again and present thin petals. In both cases they are well faceted and with truly hierarchical structures.

In Fig. 2(f), the ZnO "flowers like" that was synthesized by DM present sharp and thin ends in each petal, whereas the ZnO "flowers like" synthesized by MDM present very sharp terminations, long and very thin petals due the pressure effect.

The depletion of building blocks, in combination with the energy required for the crystal growth and the polar property change the velocity growth relation and explains the prismatic termination of the petals, in our case $V[0001] > V[01\bar{1}1] > V[01\bar{1}0]$, This is in agreement
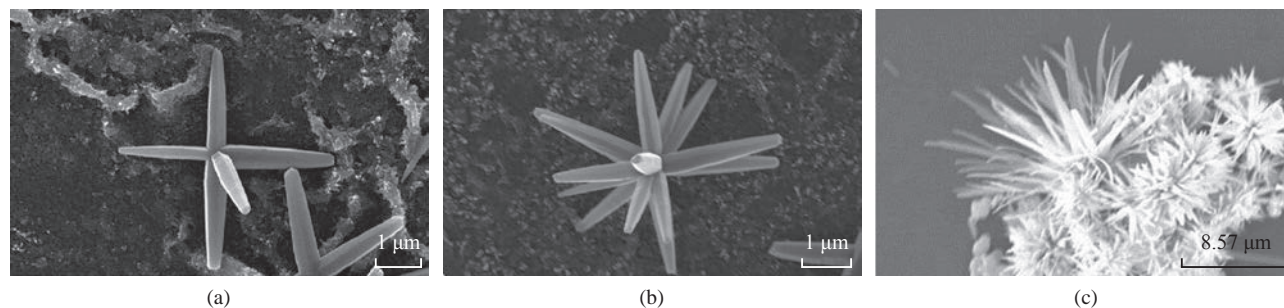
92

Nano Biomed. Eng., 2018, Vol. 10, Iss. 1

Fig. 3 Scanning electron micrographs of zinc oxide " flowers like" synthesized by **(a)** modified sequential nucleation growth method, **(b)** two steps of nucleation, and **(c)** four steps of nucleation and by modified direct method.

with the idealized growth habit reported by Li et al. [42].

The increment in the pressure increases the mobility of the building blocks ZnO(OH)⁻ and then accelerates the condensation process. The polar condition of the crystal promotes higher accumulation along the c axis V[0001], which explains the sharp termination of petals observed in the ZnO "flowers like" synthesized by MDM.

The crystalline phase presented for all ZnO "flowers like" synthesized by SNGM, MSNGM, DM and MDM is the wurzite structure (hexagonal with space group P_63mc), as was confirmed by XRD. The corresponding XRD pattern for ZnO "flowers like" synthesized by SNGM is presented in Fig. 4. All diffraction peaks were indexed and are in agreement with JCPDS 36-1451. From these patterns, lattice parameters were calculated, obtaining a = 3.253 Å and c = 5.210 Å for ZnO "flowers like" by SNGM and a = 3.251 Å and c = 5.209 Å for ZnO "flowers like" by DM. These values are in agreement with the standard parameters for the wurzite crystalline structure, a = 3.253 Å and c =
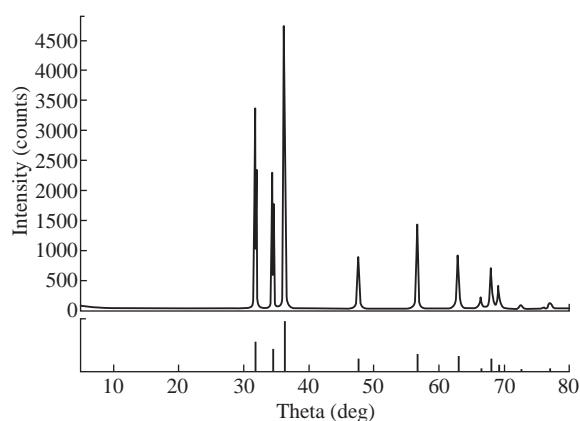
5.213 Å. From here EDS analysis showed that only Zn and O atoms are present in all the ZnO "flowers like" synthesized by the above mentioned methods; no other element was observed.

The XPS analysis was performed in order to investigate the chemical composition on the surfaces of the ZnO "flowers like" synthesized by all methods. The results showed an oxygen deficiency of atoms bonded with Zinc from 21% to 25%. The oxygen deficiencies were for DM 28%, MSNGM 25%, MDM 22% and SNGM 21%, respectively. These results could be due to the pressure effects and the variation in composition of the reaction solutions, during the synthesis processes.

Characteristic TEM, HAADF and HRTEM, images are shown in Fig. 5. In this figure, the thin and sharp termination of the petals was confirmed in the ZnO flower like synthesized by DM. The TEM and HAADF images do not show any staking defects in the crystalline structure, suggesting the good quality of the crystals.

Discussion

When nanoparticles are applied as the seeds, nanocrystal orientation and alignment could be accomplished through competition. Since the nuclei (or the seeds) are generally not well aligned on the substrate, the new crystal growth from these seeds will have no preferred orientation initially. However, as the crystals, such as nanorods, grow along the favoured crystal planes, those that are not aligned normal to the substrate are soon impeded by neighbouring crystals, and do not have room for further growth. Only the crystals with the growth orientation normal to the substrate can continue to grow, thus forming the oriented arrays. The size and population density of the seeds on the substrate primarily determines the size
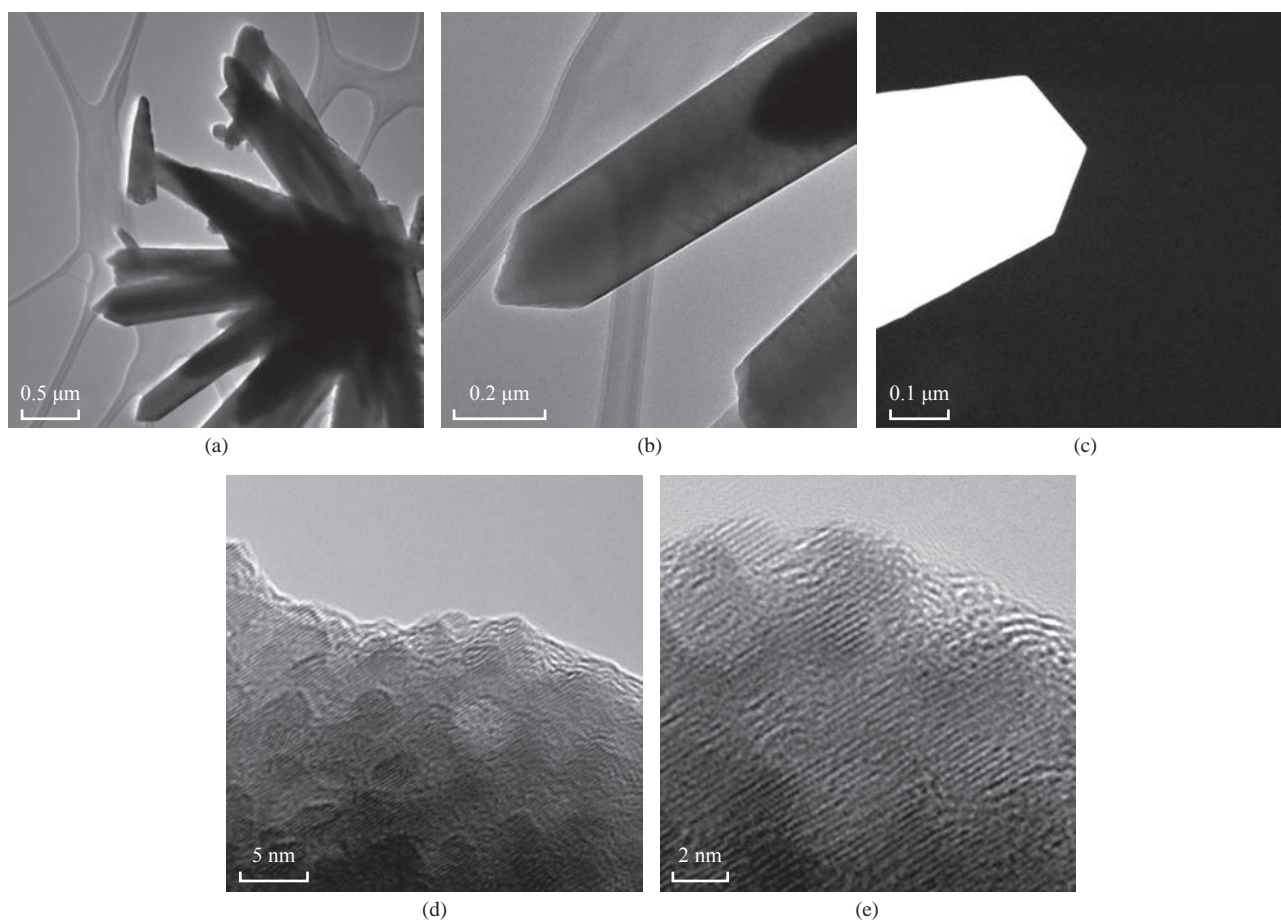

Fig. 4 X-ray diffraction pattern for the sample synthesized by SNGM.

Nano Biomed. Eng., 2018, Vol. 10, Iss. 1

93

Fig. 5 (a) TEM image of ZnO "flower like" and **(b)** TEM image of the petal. **(c)** HAADF image of the termination of the petal. **(d)** HRTEM image at 5 nm magnification and **(e)** HRTEM image at 2 nm magnification of ZnO "flower like" synthesized by DM.

and population density of the oriented nanocrystals. ZnO nanorod arrays of highly uniform orientation were produced from epitaxial growth on <0001>-oriented seed layers.

The fundamental advantage of seeded growth is the enhanced control imparted by separating nanoparticle film nucleation and oriented rod growth into two steps. In each step, different experimental conditions can be used to optimize and control each one independently. Extending this concept, we have used several synthesis steps to produce oriented nanostructures that are much more complex than simple nanorod architectures.

High-quality crystallinity, orientation alignment, and high surface/volume ratios are all important for efficient electron and photon transport in applications such as photovoltaics and lasers. With ZnO, large nanorod arrays of exceptional uniformity, orientation alignment, and optical properties (negligible defect emission) have been produced by the aqueous solution route.

The morphology evolution characteristics of ZnO nanostructures were systematically studied from dense rods to ZnO flowers like. The ZnO flowers like were prepared by direct decomposition of a $Zn(OH)_4^{2-}$ precursor and by the sequential nucleation and growth method consisted of a multistep synthesis of complex nanostructured films. The first step was to create nucleation sites, via processes such as seed deposition. After nucleation process, oriented nanocrystals grow in the 001 direction from these nucleation sites.

Conclusions

Systematical condition-dependent experiments were compared to reveal the formation and detailed growth process of ZnO nanosized crystallites and aggregates. The experimental results studied by XRD, TEM and SEM indicated that the precursor, solution basicity, reaction temperature and pressure as well as time were responsible for the variations of the morphologies. ZnO flowers like and large nanorods of exceptional uniformity, orientation alignment and optical properties were produced in this work. From XRD patterns, lattice

94

Nano Biomed. Eng., 2018,Vol. 10, Iss. 1

parameters were calculated, obtaining a = 3.253 Å and c = 5.210 Å for ZnO "flowers like" by SNGM and a = 3.251 Å and c = 5.209 Å for ZnO "flowers like" by DM. These values are in agreement with the standard parameters for the wurzite crystalline structure, a = 3.253 Å and c = 5.213 Å. From here, EDS analysis showed that only Zn and O atoms are present in all the ZnO "flowers like"; no other element was observed.

Acknowledgments

Conflict of Interests

The authors declare that no competing interest exists.

References

[1]   Z.W. Pan, Z.R. Dai, and Z.L. Wang, Nanobelts of semiconducting oxides. *Science,* 2001, 291: 1947-1949.

[2]   H. Rensmo, K. Keis, H. Lindstrom, et al., High light-to-energy conversion efficiencies for solar cells based on nanostructured ZnO electrodes. *J. Phys.Chem. B*, 1997, 101: 2598-2601.

[3]   M.A. Chamjangali, S. Boroumand, Synthesis of flower-like Ag-ZnO nanostructure and its application in the photodegradation of methyl orange. *J. Braz. Chem. Soc.*, 2013, 24: 1329-1338.

[4]   M. Huang, S. Mao, H. Feick, et al., Room-temperature ultraviolet nanowire nanolasers. *Science,* 2001, 292: 1897-1899.

[5]   M. Iwasaki, Y. Inubushi, and S. Ito, New route to prepare ultrafine ZnO particles and its reaction mechanism. *J. Mater. Sci. Lett.*, 1997, 16: 1503-1505.

[6]   D. Jezequel, J. Guenot, N. Jouini, et al., Submicrometer zinc oxide particles: Elaboration in polyol medium and morphological characteristics. *J. Mater. Res.*, 1995, 10: 77-83.

[7]   O. Milosevic, D. Uskokovic, Synthesis of BaTiO3 and ZnO varistor precursor powders by reaction spray pyrolysis. *Mater. Sci. Eng. A*, 1993, A168: 249-252.

[8]   D.R. Chen, X. Jiao, and G. Cheng, Hydrothermal synthesis of zinc oxide powders with different morphologies. *Solid State Commun.*, 2000, 113: 363-366.

[9]   C.H. Lu, C.H. Yeh, Influence of hydrothermal conditions on the morphology and particle size of zinc oxide powder. *Ceram. Int.*, 2000, 26: 351-357.

[10] T. Sekiguchi, S. Miyashita, K. Obara, et al., Hydrothermal growth of ZnO single crystals and their optical characterization. *J. Cryst. Growth*, 2000, 214/215: 72-76.

[11] B. Cheng, E.T. Samulski, Hydrothermal synthesis of one-dimensional ZnO nanostructures with different aspect ratios. *Chem. Commun.*, 2004, 8: 986-987.

[12] J.M. Wang, L. Gao, Wet chemical synthesis of ultralong and straight single-crystalline ZnO nanowires and their excellent UV emission properties. *J. Mater. Chem.*, 2003, 13: 2551-2554.

[13] Q.C. Li, V. Kumar, Y. Li, et al., Fabrication of ZnO nanorods and nanotubes in aqueous solutions. *Chem. Mater.*, 2005, 17: 1001-1006.

[14] Z. Wang, X. Qian, J. Yin, et al., Large-scale fabrication of tower-like, flower-like, and tube-like ZnO arrays by a simple chemical solution route. *Langmuir*, 2004, 20: 3441-3448.

[15] R.A. McBride, J.M. Kelly, and D.E. McCormack, Growth of well-defined ZnO microparticles by hydroxide ion hydrolysis of zinc salts. *J. Mater. Chem.*, 2003, 13: 1196-1201.

[16] Y. Zhang, H.B. Jia, X.H. Luo, et al., Synthesis, microstructure, and growth mechanism of dendrite ZnO nanowires. *J. Phys. Chem. B*, 2003, 107: 8289-8293.

[17] J.P. Liu, X.T. Huang, Y.Y. Li, et al., Large-scale synthesis of flower-like ZnO structures by a surfactant-free and low-temperature process. *Mater. Chem. Phys.*, 2006, 98: 523-527.

[18] X.D. Gao, X.M. Li, and W.D. Yu, Flowerlike ZnO nanostructures via hexamethylenetetramine-assisted thermolysis of zinc-ethylenediamine complex. *J. Phys. Chem. B*, 2005, 109: 1155-1161.

[19] T.L. Breen, J. Tien, S.R.J. Oliver, et al., Design and self-assembly of open, regular, 3D mesostructures. *Science*, 1999, 284: 948-951.

[20] R.F. Service, How far can we push chemical self-assembly? *Science*, 2005, 309: 95.

[21] J.S. Hu, Y.G. Guo, H.P. Liang, et al., Three-dimensional self-organization of supramolecular self-assembled porphyrin hollow hexagonal nanoprisms. *J. Am. Chem. Soc.*, 2005, 127: 17090-17095.

[22] G.M. Whitesides, M. Boncheva, Beyond molecules: Self-assembly of mesoscopic and macroscopic components. *Proc. Natl. Acad. Sci.*, 2002, 99: 4769-4774.

[23] K. Govender, D.S. Boyle, P.B. Kenway, et al., Understanding the factors that govern the deposition and morphology of thin films of ZnO from aqueous solution. *J. Mater. Chem.*, 2004, 14: 2575-2591.

[24] W. Zhang, X. Wen, and S. Yang, Controlled reactions on a copper surface: Synthesis and characterization of nanostructured copper compound films. *Inorg. Chem.*, 2003, 42: 5005-5014.

[25] W. Zhang, X. Wen, S. Yang, et al., Single-crystalline scroll-type nanotube arrays of copper hydroxide synthesized at room temperature. *Adv. Mater.*, 2003, 15: 822-825.

[26] L. Zhang, J. Yu, M. Mo, et al., A general solution-phase approach to oriented nanostructured films of metal chalcogenides on metal foils: The case of nickel sulphide. *J. Am. Chem. Soc.*, 2004, 126: 8116-8117.

[27] H. Hou, Y. Xie, and Q. Li, Large-Scale synthesis of single-crystalline quasi-aligned submicrometer CuO ribbons. *Cryst. Growth Des.*, 2005, 5: 201-205.

[28] Y. Li, Z. Wang, X. Ma, et al., Large-scale Cd*X* (*X*=S, Se) microtube arrays on glass substrate: transformation of CdOHCl microrod arrays by a simple template-sacrificing solution method. *J. Solid State Chem.*, 2004, 177: 4386-4393.

[29] S. Peulon, D. Lincot, Mechanistic study of cathodic electrodeposition of zinc oxide and zinc hydroxychloride films from oxygenated aqueous zinc chloride solutions. *J. Electrochem. Soc.*, 1998, 145: 864-874.

[30] R. Konenkamp, K. Boedecker, M.C. Lux-Steiner, et al., Thin film semiconductor deposition on free-standing ZnO columns. *Appl. Phys. Lett.*, 2000, 77: 2575-2577.

[31] M. Wong, A. Berenov, X. Qi, et al., Electrochemical growth of ZnO nano-rods on polycrystalline Zn foil. *Nanotechnology*, 2003, 14: 968-973.

Nano Biomed. Eng., 2018,Vol. 10, Iss. 1

95

[32] M. Izaki, T. Omi, Transparent zinc oxide films prepared by electrochemical reaction. *Appl. Phys. Lett.*, 1996, 68 : 2439-2440.

[33] B. Canava, D. Lincot, Nucleation effects on structural and optical properties of electrodeposited zinc oxide on tin oxide. *J. Appl. Electrochem.*, 2000, 30: 711-716.

[34] R. Liu, A.A. Vertegel, E.W. Bohannan, et al., Epitaxial electrodeposition of zinc oxide nanopillars on single-crystal gold. *Chem. Mater.*, 2001, 13: 508-512.

[35] R. Liu, F. Oba, E.W. Bohannan, et al., Shape control in epitaxial electrodeposition: Cu2O nanocubes on InP(001). *Chem. Mater.*, 2003, 15: 4882-4885.

[36] M.J. Siegfried, K.S. Choi, Electrochemical crystallization of cuprous oxide with systematic shape evolution. *Adv. Mater.*, 2004, 16: 1743-1746.

[37] M. Maosong, J.C. Yu, L. Zhang, et al., Self-assembly of ZnO nanorods and nanosheets into hollow microhemispheres and microspheres. *Adv. Mater.*, 2005, 17: 756-760.

[38] Z. Wang, X. Qian, J. Yin, et al., Large-scale fabrication of tower-like, flower-like, and tube-like ZnO arrays by a simple chemical solution route. *Langmuir*, 2004, 20: 3441-3448.

[39] X. Gao, X. Li, and W. Yu, Flowerlike ZnO nanostructures via hexamethylenetetramine-assisted thermolysis of zinc-ethylenediamine complex. *J. Phys. Chem. B*, 2005, 109: 1155-1161.

[40] A. Jackson, J. Vincent, and R. Turner, The mechanical design of nacre. *Proc. R. Soc. London Ser. B*, 1988, 234: 415-440.

[41] S. Yamabi, H. Imai, Growth conditions for wurtzite zinc oxide films in aqueous solutions. *J. Mater. Chem.*, 2002, 12: 3773-3778.

[42] W.J. Li, E.W. Shi, W.Z. Zhong, et al., Growth mechanism and growth habit of oxide crystals. *J. Cryst. Growth*, 1999, 203: 186-196.

[43] K. Bustos, A. Martinez, G. Martinez, et al., Covalently bonded chitosan on graphene oxide via redox reaction. *Materials*, 2013, 6: 911-926.

[44] G. Hernandez, F. Rojas, and V.M. Castaño, Ordered SiO$_2$-(phenolic-formaldehyde resin) in situnanocomposites. *Nanotechnology*, 2003, 15: 98-103.

[45] R.C. Desai, R. Kapral, *Dynamics of self-organized and self-assembled structures*. Cambridge University Press, 2009.

[46] W. Brostow, H.E. Hagg-Lobland, *Materials: Introduction and applications*. John Wiley & Sons, 2017.

[47] M.D. Bermudez, W. Brostow, F.J. Carrion-Vilches, et al., Scratch resistance of polycarbonate containing ZnO nanoparticles: Effects of sliding direction. *J. Nanosci. & Nanotech.*, 2010, 10: 6683-6686.